sustainability

MDPI

Article

Numerical Simulation Study on Lining Damage of Shield Tunnel under Train Load

Feifei Wang [1], Jinggan Shao [1,*], Wenkai Li [1], Longfei Wang [2], Yafei Wang [1] and Honglin Liu [3]

[1] Henan JiaoYuan Engineering Technology Group Co., Ltd., Zhengzhou 450001, China
[2] Henan Zhongtu Construction Engineering Co., Ltd., Zhumadian 463000, China
[3] Henan Transport Investment Group Co., Ltd., Zhengzhou 450016, China
* Correspondence: shaojingganhnjy@163.com

Abstract: Under the long-term dynamic load influence of trains, shield tunnel structures are damaged. With the increase in operating number, cumulative damage gradually increases. When cumulative damage increases to a certain value, the tunnel lining produces cracks and loses tensile strength, which leads to tunnel deformation, damage, etc. In serious cases, the tunnel ceases operation, causing traffic accidents and casualties. Based on the finite element software ABAQUS, this paper analyses the change rule of tunnel lining damage under long-term dynamic train load and explores the influence of tunnel buried depth on the change rule of tunnel lining damage. The excitation force function is used to generate a series of dynamic and static loads superimposed by sine functions to simulate the dynamic loads of trains. Load is applied above the tunnel by writing DLOAD subprogram. The results show that the damage of tunnel lining mainly occurs at the arch foot and the structural damage in other places can be neglected. Under the same loading condition, the greater the tunnel lining damage is. Under the same loading conditions, the tunnel lining damage increases with the increase in buried depth. According to the test results, the mathematical expressions of cumulative damage value versus loading times at the location prone to fatigue damage. It provides theoretical reference for safety evaluation and protection of tunnel structure under long-term train load.

Keywords: long-term load; dynamic load; shield tunnel; accumulated damage; numerical simulation

Citation: Wang, F.; Shao, J.; Li, W.; Wang, L.; Wang, Y.; Liu, H. Numerical Simulation Study on Lining Damage of Shield Tunnel under Train Load. *Sustainability* **2022**, *14*, 14018. https://doi.org/10.3390/su142114018

Academic Editors: Rui Pang, Binghan Xue, Yantao Zhu and Xiang Yu

Received: 17 September 2022
Accepted: 20 October 2022
Published: 27 October 2022

1. Introduction

With the continuous development of social levels, the scale and quantity of transportation infrastructure in China is showing a growing trend [1]. As an engineering building of underground passage, tunnel has some incomparable advantages over other projects. It shows a very obvious growth trend, as evidenced by the increasing mileage. Extra-long tunnels are emerging, and the number of shield tunnels is increasing [2,3]. The shield tunneling method exists mainly to obtain the stability of the excavation surface by balancing the earth pressure and water pressure of shield tunneling and its interior or mud pressure with that of the excavation surface. At the same time, the surrounding strata of the tunnel are supported by a strong shield shell for excavation and lining inside the shield. The design of a shield tunnel mainly includes segment design, shield type selection, structural design, etc. Safety evaluation and protection of shield tunnels in operation period has become a hot issue today [4–6]. Long-term dynamic train load causes tunnel damage. When the damage exceeds a certain limit, the lining structure is damaged, and tunnel operation safety is potentially at risk. Therefore, studying the damage of tunnel structures under long-term dynamic train load is of great significance.

The numerical simulation method is usually used to study the damage of lining structures during tunnel operation. Most tunnel lining damage is caused by external loads, such as train load, explosion load, and earthquake load. Feldgun et al. [7] studied the propagation of explosive shock waves in the air of tunnels and their interaction with the lining. Osinov et al. [8] considered the possibility of zero absolute pore pressure and

solved it using a two-dimensional plane strain formula of a finite element program to study the dynamic deformation of tunnel lining and soil caused by medium-amplitude pressure pulses caused by an explosion in the tunnel. After verifying the consistency of the finite element simulation results with experimental model results, Keskin et al. [9] used a finite element method (FEM) to study the behavior of an underground circular tunnel under an impact load caused by surface explosion, and further verified that the pressure curves obtained from the concrete lining and embedded reinforcement cage during the explosion were almost the same. The explosion load and earthquake load are relatively rare in the daily operation of a tunnel, while the train load exists for a long time during tunnel operation. At present, many scholars have studied the mechanical response of tunnel structures under train load [10–13]. Huang et al. [14] used the railway-coupler-tunnel-subgrade model to evaluate the train vibration load, and then applied it to the track bed to simulate the movement of a subway train using a 3D model. A cyclic flow model was introduced in the numerical analysis to simulate the mechanical behavior of saturated soft clay. Train settlement of a subway tunnel in saturated clay was studied by means of a soil–water fully-coupled dynamic finite element method (FEM). The feasibility of the proposed numerical method in evaluating the train settlement was verified by simulating the vibration of the trial-running train with 2D and 3D models. Wang et al. [15] used the three-dimensional finite element method to study the initial stress state and dynamic response characteristics of tunnel lining during operation, and also used a set of indoor fatigue test equipment independently developed to study the damage evolution characteristics of tunnel invert under dynamic load and initial static load. Wu et al. [16] studied the stress distribution pattern in the subsoil around the tunnel caused by train motion based on a simplified mechanical model. In this model, the effects of rails, connecting bolts, ballasts, lining and foundations are considered. The initial and dynamic stress states of subsoil caused by train loading were obtained using a two-dimensional finite element calculation. Combined with the empirical equation, the cumulative plastic strain of the foundation and the long-term settlement of the tunnel were obtained. Li et al. [17] studied that under the combined influence of heavy-haul trains and groundwater, the surrounding rock particles gradually become loose under the dynamic influence of heavy-haul trains due to the void mechanism of surrounding rock at the bottom of tunnel. This is particularly obvious in the defective location of weak surrounding rock, at the same time, the increase in axle load and deterioration of surrounding rock condition will aggravate the situation of the tunnel bottom cavity. Di et al. [18] proposed an improved tunnel model to evaluate the dynamic stress caused by trains in saturated soil, which can consider various moving loads, grouting layers, and pore water pressure. Based on the actual parameters of train speed, tunnel, grouting layer and soil mass of the Shanghai Metro, the spatial distribution of dynamic stress of soil mass and stress state at different locations under the moving load of train were analyzed. Kanik et al. [19,20] selected the best tunnel support scheme by using rock mass rating (RMR), rock mass quality (Q), and rock mass index (RMi) evaluation indexes. Regarding the long-term influence of train load, little research has been conducted on the regularity of the damage degree of tunnel lining at different buried depths. With the increase in loading times, the change rule of tunnel lining damage needs to be further studied. Ma et al. [21] tested the dynamic behavior of a tunnel basement structure with axial load. By analyzing the dynamic response and the influence law of fatigue life of heavy-duty train under different base conditions (complete, damaged, and repaired), the adaptability of railway tunnel equipment to freight truck axle load was clarified. Yan et al. [22] proposed an improved constitutive model of concrete under uniaxial cyclic load considering the fatigue rigidity degradation, fatigue strength degradation, and fatigue residual strain increment of concrete. According to this constitutive model, the dynamic response and accumulated damage of tunnel cross structure under different train operating years were analyzed. Maleska et al. [23,24] explored the influence of different cover depths on the stress and strain of underground culvert structure based on finite element method. The above scholars did not consider the long-term train load in their

studies on underground structures such as tunnels. Under the long-term influence of train load, there is little research on the damage degree variation law of tunnel lining at different buried depths. With the increasing number of train loads, the change law of tunnel lining damage needs to be studied further.

In this paper, based on the finite element analysis method, the excitation force function was used to generate a series of sinusoidal functions to superimpose dynamic and static loads to simulate the dynamic loads of trains. Through the analysis of damage variation law of shield tunnel lining under long-term dynamic loads under different buried depths, the empirical formula of accumulated damage of tunnel concrete structure under dynamic loads of trains is provided. It provides theoretical reference for safety evaluation and safety protection research of shield tunnel under long-term dynamic train load.

2. Tunnel Numerical Model and Train Load

In a silty sand layer, the inner diameter of a shield tunnel is 6 m, and the lining thickness is 0.3 m. The width of the tunnel track bed is 5.2 m, and the maximum thickness is 1.5 m. In the tunnel calculation model, the rail section is simplified to a rectangle with a height of 0.2 m and a width of 0.11 m. In order to explore the influence of tunnel buried depth on tunnel lining damage, two independent shield tunnel models with 15 and 20 m buried depth are established, respectively. The schematic diagram of the shield tunnel model based on ABAQUS 6.14 finite element software is shown in Figures 1 and 2, and the section perpendicular to the center axis of the tunnel is 50 m × 50 m square, the length of the model along the axis of the tunnel is 30 m, and the horizontal distance between the rail and the axis is 0.7175 m. In the coupled dynamic finite element model, the formation is simplified as an isotropic, homogeneous elastic medium. The Mohr-Coulomb model is used for the soil mass of the tunnel. The soil mass with a density of 1860 kg/m^3, and the elastic modulus is 20 MPa. The internal friction angle, cohesion and Poisson ratio of soils are 30°, 0 kPa, and 0.27 respectively. The C50 concrete damage model (CDP model) is used for lining and ballast of tunnel in the calculation model. The rail adopts an elastic model with a density of 7850 kg/m^3, and the elastic modulus is 210 GPa. The Poisson ratio of the rails is 0.25. Elastic models are used for outsourcing polymers. The density of polymer material is 600 kg/m^3, elastic modulus is 300 MPa and Poisson ratio is 0.35. The Friction coefficient between tunnel and soil is 0.55. The viscoelastic boundary is applied at the truncated boundary to eliminate the reflection effect of the boundary on the incident wave. Load application is achieved by writing DLOAD subprogram. The subprogram is used to simulate the long-term effects of train loads during calculation.

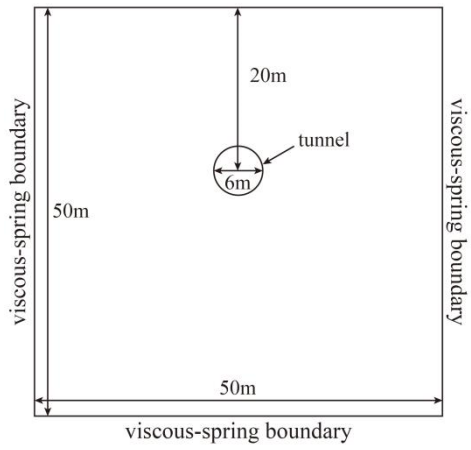

Figure 1. Plane diagram of finite element model.

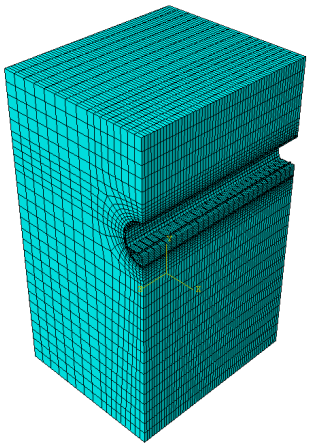

Figure 2. Schematic diagram of 3D finite element model.

Hashash et al. [25–27] explored the stress-strain characteristics of infrastructures such as subways, railways, and highways under typical static and dynamic loads. The dynamic load of the train is simulated by the excitation force function, including the dynamic load and static load superimposed by a series of sinusoidal functions:

$$F_t = A_u + A_1 \sin \omega_1 t + A_2 \sin \omega_2 t + A_3 \sin \omega_3 t \quad (1)$$

In Formula (1), A_u is the static load of the wheel, A_1, A_2, and A_3 are the peak values of vibration load corresponding to vibration frequencies ω_1, ω_2, and ω_3. Referring to the research results of Pan and Pande [28], the values of A_u, A_1, A_2, and A_3 are 150, 150, 160, and 240 kN respectively, and the values of ω_1, ω_2, and ω_3 are 25, 100, and 250 rad/s respectively.

The waveform diagram of the train load is shown in Figure 3.

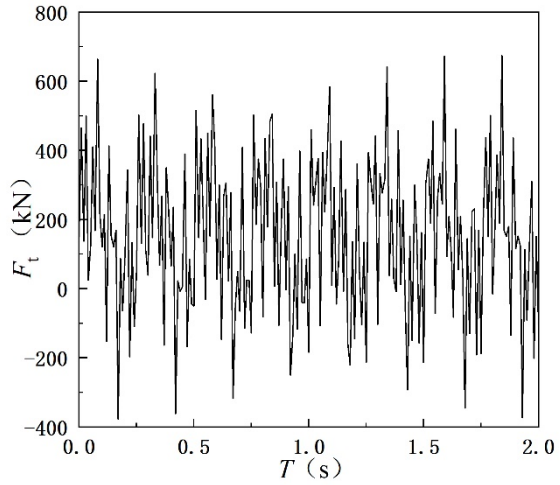

Figure 3. Dynamic load waveform diagram.

3. Calculation Results

The tunnel model is symmetrical in structure, and selecting one-half of the tunnel model along the middle line of the tunnel as the analysis object can improve calculation efficiency. In order to analyze the damage distribution law of the shield tunnel under the influence of train vibration load, the damage calculation results of different locations around the tunnel were selected and compared. Due to the symmetrical structure of the tunnel, only 6 position points are selected uniformly on the left side of the tunnel. The arch bottom of the tunnel is position point 1, the arch foot of the tunnel is position point 2, the

arch waist of the tunnel is position point 3, the arch shoulders of the tunnel are position points 4 and 5, and the vault of the tunnel is position point 6, as shown in Figure 4.

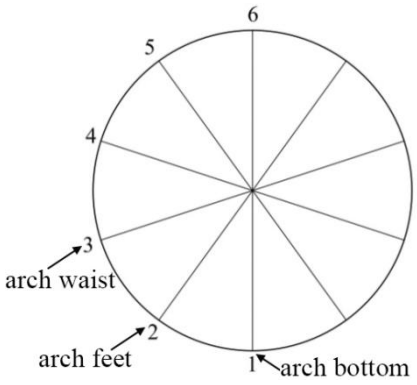

Figure 4. Schematic diagram of analysis position distribution.

3.1. Variation Regularity of Tunnel Cumulative Damage

The variation rule of accumulated damage at each analyzed position of the tunnel is shown in Figure 5 when the buried depth of the central axis of the tunnel is 20 m. As can be seen from Figure 5, the cumulative damage value at position 2 and position 3 show an increasing trend with the increase in loading times, and the growth rate of cumulative damage gradually increases with the increase in loading times. The trend of tunnel damage increases exponentially. The accumulated damage at position 2 increased the fastest. The accumulated damage reaches 0.911 when the number of loads reach 1.13 million. The accumulated damage value of tunnel surface lining exceeds 0.9 and the structure has been destroyed. The cumulative damage growth rate at position 3 is smaller than that at position 2, and the cumulative damage reaches 0.509 when the loading times reach 1.13 million. This phenomenon occurs because the loading position of the train is the middle and lower part of the tunnel, and the load at position 3 is less than that at position 2 after decomposition. The bearing foundation exists at position 1 and the load at position 2 is the largest. The variation of accumulated damage of tunnel lining with increasing loading times is shown in Figure 5. The cumulative damage at positions 1, 4, 5, and 6 also tends to increase with the increase in loading times, but it can be seen from the numerical value that the cumulative damage increases slightly with respect to positions 2 and 3. The reason for this phenomenon is that the damage of the lower lining of the tunnel is caused by multiple factors such as the upper soil pressure, which belongs to the normal range and can be ignored. It can be concluded from Figure 5 that lining damage mainly occurs at the arch foot under train load, which is consistent with the research conclusions of other scholars [16,17].

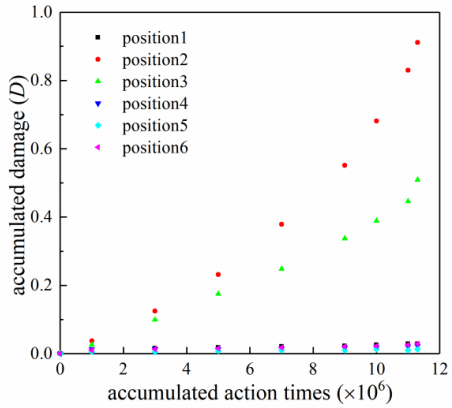

Figure 5. Variation regularity of cumulative damage at different analysis locations with tunnel buried depth of 20 m.

The variation rule of accumulated damage at each analyzed position of the tunnel is shown in Figure 6 when the buried depth of the tunnel is 15 m. The damage at position 2 also increased the fastest. The cumulative damage reached 0.907 when the loading times reached 1.16 million times. The accumulated damage of tunnel lining exceeded 0.9 and the lining structure was destroyed. The cumulative damage value at position 3 reached 0.507 when the loading times were at 1.16 million times. It can be seen from Figures 5 and 6 that when the loading times reach 1.16 million and the buried depth is 20 m, the accumulated damage of tunnel lining at positions 2 and 3 are 0.911 and 0.509, respectively. The accumulated damage of the tunnel lining at positions 2 and 3 are 0.907 and 0.507, respectively, when the buried depth of the tunnel is 15 m. From a numerical point of view, the damage value of the tunnel lining changes slightly when the buried depth of the tunnel is 15 and 20 m; however; it can't be ignored. By comparing the change rule of accumulated damage of tunnel lining with different buried depths, it can be concluded that under the same loading condition, the accumulated damage of tunnel lining is larger when the tunnel buried depth is larger, and the corresponding fatigue life is shorter. Therefore, when inspecting and repairing the tunnel lining, more attention should be paid to the tunnel with deeply buried depth, and the inspection times should be increased to ensure the normal and safe operation of the tunnel.

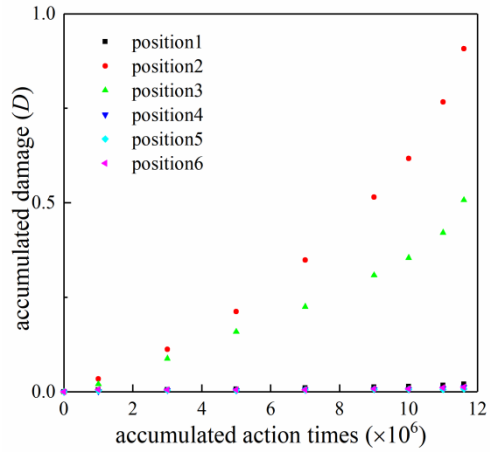

Figure 6. Variation regularity of cumulative damage at different analysis locations with tunnel buried depth of 15 m.

3.2. Cumulative Damage Change Rule and Fitted Curve at Position 2

According to the numerical calculation results, the accumulated damage at position 2 is the most significant under the influence of train load. The cumulative damage values at position 2 under different loading times are fitted. According to the variation rule of cumulative damage, the fitting formula [16] is:

$$D = Ae^{Bx} + C \quad (2)$$

In Formula (2), A, B and C are all fitting parameters, and x is the cumulative influence times.

The fitting results under different tunnel depths are shown in Figures 7 and 8 and Table 1.

The fitting results show that R^2 exceeds 0.99 under both operating conditions and the fitting degree is high.

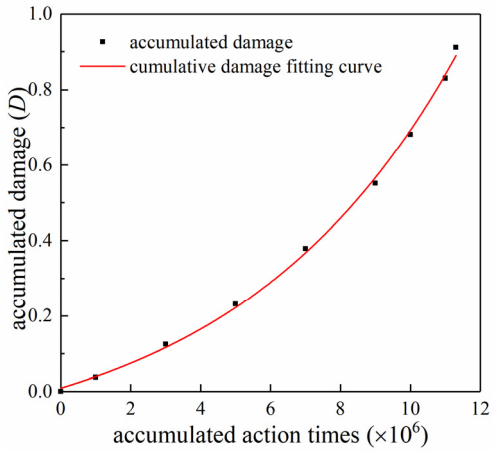

Figure 7. Accumulated damage at location 2 and fitted curve at 20 m buried depth of tunnel central axis.

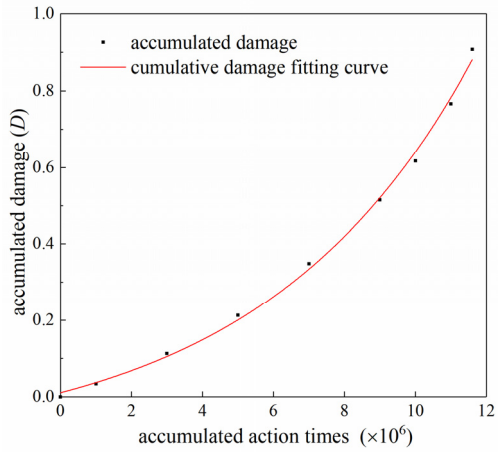

Figure 8. Accumulated damage at location 2 and fitted curve at 15 m buried depth of tunnel central axis.

Table 1. Fitting results of accumulated damage of tunnel lining.

Buried Depth of Tunnel Centre Axis/m	*A*	*B*	*C*	R^2 (Coefficient of Determination)
20	0.178	0.158	−0.169	0.998
15	0.143	0.169	−0.131	0.999

4. Conclusions

In this paper, the dynamic load of a train is simulated by establishing an excitation force function. Based on ABAQUS finite element software, the development law of shield tunnel lining damage under long-term train load is calculated and analyzed. Based on the test results, the cumulative damage development law at the locations prone to fatigue failure is fitted by empirical formula, and the variation law of cumulative damage of tunnel lining under different tunnel burial depths are compared and analyzed. The main conclusions are as follows:

- With the increase in loading times, the accumulated damage value of lining located at the arch foot and arch waist of the tunnel shows an increasing trend, and the accumulated damage growth rate of lining at the arch foot is the highest. Damage to tunnel lining at the arch foot occurs when loading times reach 1.16 million;
- Under influence of long-term train load, the tunnel lining at the arch foot is most prone to fatigue damage, followed by the arch waist. The accumulated damage value at the tunnel arch foot exceeds 0.9 and the tunnel arch waist exceeds 0.5 under different

buried depths when loading times reach 1.16 million. Accumulated damage at other locations is negligible;

- The cumulative damage value of the lining at the arch foot and arch waist of the shield tunnel increases exponentially with the increase in loading times. The fastest change rate in accumulated damage value of the tunnel lining occurs at the arch foot;
- Under the same loading conditions, the cumulative damage of the tunnel lining is proportional to the buried depth of the tunnel. Under the influence of train load, the accumulated damage of the tunnel lining decreases continuously as the buried depth of the tunnel decreases. The corresponding tunnel structure with smaller buried depth has a longer service life. For deeply buried tunnels, the number of routine tunnel inspections and maintenances should be increased to ensure the normal and safe operation of tunnels.

Author Contributions: Investigation, Y.W.; Methodology, W.L.; Software, L.W.; Visualization, H.L.; Writing—original draft, J.S.; Writing—review & editing, F.W. All authors have read and agreed to the published version of the manuscript.

Funding: This research received no external funding.

Informed Consent Statement: Informed consent was obtained from all individual participants included in the study.

Data Availability Statement: The raw data supporting the conclusion of this article will be made available by the authors, without undue reservation.

Conflicts of Interest: The authors declare no conflict of interest.

References

1. Lin, S.; Zhou, Z.; Xi, Y. Model-Based Traffic Congestion Control in Urban Road Networks: Analysis of performance criteria, Transportation research record. *Transp. Res. Rec. J. Transp. Res. Board* **2013**, *2390*, 112–120. [CrossRef]
2. Zhou, S.; Ye, G.-L.; Han, L.; Jian-Hua, W. Key Construction Technologies for Large River-Crossing Slurry Shield Tunnel: Case Study. *J. Aerosp. Eng.* **2021**, *34*, 04020118. [CrossRef]
3. Wei, L.I.; Chuan, H.E. Mechanics analysis and structure design of river-crossing shield tunnel of super-large section. *China J. Highw. Transp.* **2007**, *20*, 76.
4. Lei, M.; Lin, D.; Huang, Q.; Shi, C.; Huang, L. Research on the construction risk control technology of shield tunnel underneath an operational railway in sand pebble formation: A case study. *Eur. J. Environ. Civ. Eng.* **2018**, *24*, 1558–1572. [CrossRef]
5. Liu, Y.; Chen, H.; Zhang, L.; Wang, X. Risk prediction and diagnosis of water seepage in operational shield tunnels based on random forest. *J. Civ. Eng. Manag.* **2021**, *27*, 539–552. [CrossRef]
6. Lyu, H.-M.; Shen, S.-L.; Zhou, A.; Yin, Z.-Y. Assessment of safety status of shield tunnelling using operational parameters with enhanced SPA. *Tunn. Undergr. Space Technol.* **2022**, *123*, 104428. [CrossRef]
7. Feldgun, V.; Karinski, Y.; Yankelevsky, D. The effect of an explosion in a tunnel on a neighboring buried structure. *Tunn. Undergr. Space Technol.* **2014**, *44*, 42–55. [CrossRef]
8. Osinov, V.A.; Chrisopoulos, S.; Triantafyllidis, T. Numerical analysis of the tunnel-soil interaction caused by an explosion in the tunnel. *Soil Dyn. Earthq. Eng.* **2018**, *122*, 318–326. [CrossRef]
9. Keskin, I.; Ahmed, M.Y.; Taher, N.R.; Gör, M.; Abdulsamad, B.Z. An evaluation on effects of surface explosion on underground tunnel; availability of ABAQUS Finite element method. *Tunn. Undergr. Space Technol.* **2021**, *120*, 104306. [CrossRef]
10. Metrikine, A.; Vrouwenvelder, A. Surface ground vibration due to a moving train in a tunnel: Two-dimensional model. *J. Sound Vib.* **2000**, *234*, 43–66. [CrossRef]
11. Deng, F.-H.; Mo, H.-H.; Zeng, Q.-J.; Yang, X.-J. Analysis of the Dynamic Response of a Shield Tunnel in Soft Soil Under a Metro-Train Vibrating Load. *J. China Univ. Min. Technol.* **2006**, *16*, 509–513. [CrossRef]
12. Sekiya, H.; Masuda, K.; Nagakura, S.; Inuzuka, S. Determination of shield tunnel deformation under train load using MEMS accelerometers. *Tunn. Undergr. Space Technol.* **2022**, *126*, 104535. [CrossRef]
13. Wang, D.; Luo, J.; Li, F.; Wang, L.; Su, J. Research on dynamic response and fatigue life of tunnel bottom structure under coupled action of train load and groundwater. *Soil Dyn. Earthq. Eng.* **2022**, *161*, 107405. [CrossRef]
14. Huang, Q.; Huang, H.-W.; Ye, B.; Zhang, D.-M.; Gu, L.-L.; Zhang, F. Dynamic response and long-term settlement of a metro tunnel in saturated clay due to moving train load. *Soils Found.* **2017**, *57*, 1059–1075. [CrossRef]
15. Wang, A.; Shi, C.; Zhao, C.; Deng, E.; Yang, W.; He, H. Response Characteristics of Cross Tunnel Lining under Dynamic Train Load. *Appl. Sci.* **2020**, *10*, 4406. [CrossRef]

16. Wu, H.-N.; Shen, S.-L.; Chai, J.-C.; Zhang, D.-M.; Xu, Y.-S. Evaluation of train-load-induced settlement in metro tunnels. *Proc. Inst. Civ. Eng.-Geotech. Eng.* **2015**, *168*, 396–406. [CrossRef]
17. Li, Z.; Li, Z.; Huang, W.; Xu, Z.; Zhang, W.; Chen, K. Tunnel Bottom Cavity Laws of Heavy-Haul Railway Tunnel under Train Load and Groundwater in Weak Surrounding Rock Condition. *KSCE J. Civ. Eng.* **2021**, *26*, 1451–1464. [CrossRef]
18. Di, H.; Zhou, S.; He, C.; Zhang, X.; Luo, Z. Three-dimensional multilayer cylindrical tunnel model for calculating train-induced dynamic stress in saturated soils. *Comput. Geotech.* **2016**, *80*, 333–345. [CrossRef]
19. Kanık, M.; Gurocak, Z.; Alemdag, S. A comparison of support systems obtained from the RMR89 and RMR14 by numerical analyses: Macka Tunnel project, NE Turkey. *J. Afr. Earth Sci.* **2015**, *109*, 224–238. [CrossRef]
20. Kanik, M.; Gurocak, Z. Importance of numerical analyses for determining support systems in tunneling: A comparative study from the trabzon-gumushane tunnel, Turkey. *J. Afr. Earth Sci.* **2018**, *143*, 253–265. [CrossRef]
21. Ma, W.; Chai, J.; Zhu, Z.; Han, Z.; Ma, C.; Li, Y.; Zhu, Z.; Liu, Z.; Niu, Y.; Ma, Z.; et al. Research on Vibration Law of Railway Tunnel Substructure under Different Axle Loads and Health Conditions. *Shock Vib.* **2021**, *2021*, 1–14. [CrossRef]
22. Yan, Q.; Xu, Y.; Zhang, W.; Geng, P.; Yang, W. Numerical analysis of the cracking and failure behaviors of segmental lining structure of an underwater shield tunnel subjected to a derailed high-speed train impact. *Tunn. Undergr. Space Technol.* **2018**, *72*, 41–54. [CrossRef]
23. Yeau, K.Y.; Sezen, H.; Fox, P.J. Simulation of Behavior of In-Service Metal Culverts. *J. Pipeline Syst. Eng. Pr.* **2014**, *5*, 158. [CrossRef]
24. Maleska, T.; Beben, D. Behaviour of soil-steel composite bridge with various cover depths under seismic excitation. *Steel Compos. Struct.* **2022**, *42*, 747–764. [CrossRef]
25. Maleska, T.; Beben, D.; Nowacka, J. Seismic vulnerability of a soil-steel composite tunnel—Norway Tolpinrud Railway Tunnel Case Study. *Tunn. Undergr. Space Technol.* **2021**, *110*, 103808. [CrossRef]
26. Flener, E.B.; Karoumi, R. Dynamic testing of a soil–steel composite railway bridge. *Eng. Struct.* **2009**, *31*, 2803–2811. [CrossRef]
27. Hashash, Y.M.; Hook, J.J.; Schmidt, B.; Yao, J.I.-C. Seismic design and analysis of underground structures. *Tunn. Undergr. Space Technol.* **2001**, *16*, 247–293. [CrossRef]
28. Pan, C.S.; Pande, G.N. Preliminary numerical analysis of train dynamic load response in loess tunnel by finite element method. *J. Civ. Eng.* **1984**, *4*, 18–28. (In Chinese)